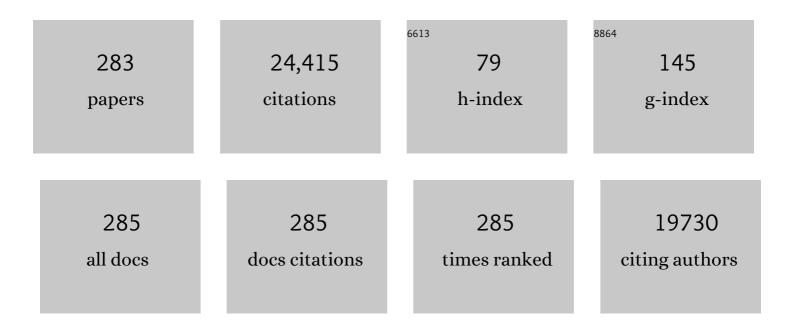
## Adriaan A Lammertsma

List of Publications by Year in descending order

Source: https://exaly.com/author-pdf/7773216/publications.pdf Version: 2024-02-01



#	Article	IF	CITATIONS
1	Whole body macrophage PET imaging for disease activity assessment in early rheumatoid arthritis. Journal of Rheumatology, 2022, , jrheum.210928.	2.0	0
2	Impact of cerebral blood flow and amyloid load on SUVR bias. EJNMMI Research, 2022, 12, 29.	2.5	6
3	Repeatability of parametric methods for [ <sup>18</sup> F]florbetapir imaging in Alzheimer's disease and healthy controls: A test–retest study. Journal of Cerebral Blood Flow and Metabolism, 2021, 41, 569-578.	4.3	10
4	Test-Retest Variability of Relative Tracer Delivery Rate as Measured by [11C]PiB. Molecular Imaging and Biology, 2021, 23, 335-339.	2.6	2
5	Strategies to reduce sample sizes in Alzheimer's disease primary and secondary prevention trials using longitudinal amyloid PET imaging. Alzheimer's Research and Therapy, 2021, 13, 82.	6.2	14
6	Education, training and registration of Medical Physics Experts across Europe. Physica Medica, 2021, 85, 129-136.	0.7	6
7	Houdini's Illusions: Some Acts Are Not What They Seem to Be. Journal of Nuclear Medicine, 2021, 62, 1832-1832.	5.0	0
8	Quantitative parametric maps of O-(2-[ <sup>18</sup> F]fluoroethyl)-L-tyrosine kinetics in diffuse glioma. Journal of Cerebral Blood Flow and Metabolism, 2020, 40, 895-903.	4.3	8
9	Parametric methods for [ <sup>18</sup> F]flortaucipir PET. Journal of Cerebral Blood Flow and Metabolism, 2020, 40, 365-373.	4.3	22
10	[11C]PIB amyloid quantification: effect of reference region selection. EJNMMI Research, 2020, 10, 123.	2.5	17
11	Quantification of [ <sup>18</sup> F]florbetapir: A test–retest tracer kinetic modelling study. Journal of Cerebral Blood Flow and Metabolism, 2019, 39, 2172-2180.	4.3	22
12	Optimized dual-time-window protocols for quantitative [18F]flutemetamol and [18F]florbetaben PET studies. EJNMMI Research, 2019, 9, 32.	2.5	31
13	Direct comparison of [11C] choline and [18F] FET PET to detect glioma infiltration: a diagnostic accuracy study in eight patients. EJNMMI Research, 2019, 9, 57.	2.5	8
14	Amyloid PET and cognitive decline in cognitively normal individuals: the SCIENCe project. Neurobiology of Aging, 2019, 79, 50-58.	3.1	41
15	Association of amyloid pathology with memory performance and cognitive complaints in cognitively normal older adults: a monozygotic twin study. Neurobiology of Aging, 2019, 77, 58-65.	3.1	14
16	Semi-quantitative cerebral blood flow parameters derived from non-invasive [ <sup>15</sup> 0]H <sub>2</sub> 0 PET studies. Journal of Cerebral Blood Flow and Metabolism, 2019, 39, 163-172.	4.3	12
17	Diagnostic Value of Transluminal Attenuation Gradient for the Presence of Ischemia as Defined by Fractional Flow Reserve and Quantitative Positron Emission Tomography. JACC: Cardiovascular Imaging, 2019, 12, 323-333.	5.3	19
18	An exploratory clinical study of p38 <i>α</i> kinase inhibition in Alzheimer's disease. Annals of Clinical and Translational Neurology, 2018, 5, 464-473.	3.7	43

#	Article	IF	CITATIONS
19	Effect of Plaque Burden and MorphologyÂon Myocardial Blood Flow andÂFractional FlowÂReserve. Journal of the American College of Cardiology, 2018, 71, 499-509.	2.8	133
20	Molecular Imaging of ABCB1 and ABCG2 Inhibition at the Human Blood–Brain Barrier Using Elacridar and <sup>11</sup> C-Erlotinib PET. Journal of Nuclear Medicine, 2018, 59, 973-979.	5.0	19
21	Cerebral rituximab uptake in multiple sclerosis: A <sup>89</sup> Zr-immunoPET pilot study. Multiple Sclerosis Journal, 2018, 24, 543-545.	3.0	19
22	[18F]NaF PET/CT scan as an early marker of heterotopic ossification in fibrodysplasia ossificans progressiva. Bone, 2018, 109, 143-146.	2.9	31
23	Hypometabolism of the posterior cingulate cortex is not restricted to Alzheimer's disease. NeuroImage: Clinical, 2018, 19, 625-632.	2.7	23
24	Imaging and Methotrexate Response Monitoring of Systemic Inflammation in Arthritic Rats Employing the Macrophage PET Tracer [ <sup>18</sup> F]Fluoro-PEG-Folate. Contrast Media and Molecular Imaging, 2018, 2018, 1-10.	0.8	17
25	Personalizing NSCLC therapy by characterizing tumors using TKI-PET and immuno-PET. Lung Cancer, 2017, 107, 1-13.	2.0	30
26	In vivo assessment of myocardial viability after acute myocardial infarction: A head-to-head comparison of the perfusable tissue index by PET and delayed contrast-enhanced CMR. Journal of Nuclear Cardiology, 2017, 24, 657-667.	2.1	13
27	Strategies towards in vivo imaging of active transglutaminase type 2 using positron emission tomography. Amino Acids, 2017, 49, 585-595.	2.7	11
28	Forward to the Past: The Case for Quantitative PET Imaging. Journal of Nuclear Medicine, 2017, 58, 1019-1024.	5.0	128
29	Synthesis, radiolabeling and preclinical evaluation of a [11 C]GMOM derivative as PET radiotracer for the ion channel of the N-methyl-D-aspartate receptor. Nuclear Medicine and Biology, 2017, 51, 25-32.	0.6	9
30	Comparison of Coronary CT Angiography, SPECT, PET, and Hybrid Imaging for Diagnosis of Ischemic Heart Disease Determined by Fractional Flow Reserve. JAMA Cardiology, 2017, 2, 1100.	6.1	324
31	Comparison of In Vitro Assays in Selecting Radiotracers for In Vivo P-Glycoprotein PET Imaging. Pharmaceuticals, 2017, 10, 76.	3.8	4
32	Quantitative agreement between [ <sup>15</sup> 0]H <sub>2</sub> 0 PET and model free QUASAR MRIâ€derived cerebral blood flow and arterial blood volume. NMR in Biomedicine, 2016, 29, 519-526.	2.8	10
33	Multiparametric Analysis of the Relationship Between Tumor Hypoxia and Perfusion with <sup>18</sup> F-Fluoroazomycin Arabinoside and <sup>15</sup> O-H <sub>2</sub> O PET. Journal of Nuclear Medicine, 2016, 57, 530-535.	5.0	13
34	Measurement of LV Volumes andÂFunction Using Oxygen-15 Water-Gated PET and Comparison With CMR Imaging. JACC: Cardiovascular Imaging, 2016, 9, 1472-1474.	5.3	15
35	Parametric Binding Images of the TSPO Ligand <sup>18</sup> F-DPA-714. Journal of Nuclear Medicine, 2016, 57, 1543-1547.	5.0	23
36	Synthesis, radiolabeling and evaluation of novel amine guanidine derivatives as potential positron emission tomography tracers for the ion channel of the N-methyl-d-aspartate receptor. European Journal of Medicinal Chemistry, 2016, 118, 143-160.	5.5	10

#	Article	IF	CITATIONS
37	Quantification of the novel <i>N</i> -methyl- <scp>d</scp> -aspartate receptor ligand [ <sup>11</sup> C]GMOM in man. Journal of Cerebral Blood Flow and Metabolism, 2016, 36, 1111-1121.	4.3	19
38	Quantitative and Simplified Analysis of <sup>11</sup> C-Erlotinib Studies. Journal of Nuclear Medicine, 2016, 57, 861-866.	5.0	22
39	Development of carbon-11 labeled acryl amides for selective PET imaging of active tissue transglutaminase. Nuclear Medicine and Biology, 2016, 43, 232-242.	0.6	29
40	Repeatability of Quantitative <sup>18</sup> F-Fluoromethylcholine PET/CT Studies in Prostate Cancer. Journal of Nuclear Medicine, 2016, 57, 721-727.	5.0	22
41	Myocardial denervation coincides with scar heterogeneity in ischemic cardiomyopathy: A PET and CMR study. Journal of Nuclear Cardiology, 2016, 23, 1480-1488.	2.1	9
42	The Association of Glucose Metabolism and Eigenvector Centrality in Alzheimer's Disease. Brain Connectivity, 2016, 6, 1-8.	1.7	18
43	Neurophysiological Effects of Sleep Deprivation in Healthy Adults, a Pilot Study. PLoS ONE, 2015, 10, e0116906.	2.5	40
44	Doppler-Derived Intracoronary Physiology Indices Predict the Occurrence of Microvascular Injury and Microvascular Perfusion Deficits After Angiographically Successful Primary Percutaneous Coronary Intervention. Circulation: Cardiovascular Interventions, 2015, 8, e001786.	3.9	55
45	Synthesis, structure activity relationship, radiolabeling and preclinical evaluation of high affinity ligands for the ion channel of the N-methyl-d-aspartate receptor as potential imaging probes for positron emission tomography. Bioorganic and Medicinal Chemistry, 2015, 23, 1189-1206.	3.0	14
46	Quantification of <sup>18</sup> F-Fluorocholine Kinetics in Patients with Prostate Cancer. Journal of Nuclear Medicine, 2015, 56, 365-371.	5.0	32
47	The Dopamine Stabilizer (â^')-OSU6162 Occupies a Subpopulation of Striatal Dopamine D2/D3 Receptors: An [11C]Raclopride PET Study in Healthy Human Subjects. Neuropsychopharmacology, 2015, 40, 472-479.	5.4	22
48	Incremental diagnostic value of epicardial adipose tissue for the detection of functionally relevant coronary artery disease. Atherosclerosis, 2015, 242, 161-166.	0.8	25
49	Quantification of [ <sup>18</sup> F]DPA-714 Binding in the Human Brain: Initial Studies in Healthy Controls and Alzheimer'S Disease Patients. Journal of Cerebral Blood Flow and Metabolism, 2015, 35, 766-772.	4.3	99
50	Cerebral perfusion and glucose metabolism in Alzheimer's disease and frontotemporal dementia: two sides of the same coin?. European Radiology, 2015, 25, 3050-3059.	4.5	80
51	Prevalence of Amyloid PET Positivity in Dementia Syndromes. JAMA - Journal of the American Medical Association, 2015, 313, 1939.	7.4	501
52	Radiopharmaceuticals for assessing ABC transporters at the blood–brain barrier. Clinical Pharmacology and Therapeutics, 2015, 97, 362-371.	4.7	25
53	Use of a Single <sup>11</sup> C- <i>Meta</i> -Hydroxyephedrine Scan for Assessing Flow–Innervation Mismatches in Patients with Ischemic Cardiomyopathy. Journal of Nuclear Medicine, 2015, 56, 1706-1711.	5.0	27
54	Comparison of Velocity- and Acceleration-Selective Arterial Spin Labeling with [ <sup>15</sup> 0]H <sub>2</sub> 0 Positron Emission Tomography. Journal of Cerebral Blood Flow and Metabolism, 2015, 35, 1296-1303.	4.3	24

#	Article	IF	CITATIONS
55	Quantification of Dynamic <sup>11</sup> C-Phenytoin PET Studies. Journal of Nuclear Medicine, 2015, 56, 1372-1377.	5.0	17
56	PET/CT-Derived Whole-Body and Bone Marrow Dosimetry of <sup>89</sup> Zr-Cetuximab. Journal of Nuclear Medicine, 2015, 56, 249-254.	5.0	40
57	Quantification of cerebral blood flow in healthy volunteers and type 1 diabetic patients: Comparison of MRI arterial spin labeling and [ <sup>15</sup> 0]H <sub>2</sub> 0 positron emission tomography (PET). Journal of Magnetic Resonance Imaging, 2014, 40, 1300-1309.	3.4	30
58	Impaired Hyperemic Myocardial Blood Flow Is Associated With Inducibility of Ventricular Arrhythmia in Ischemic Cardiomyopathy. Circulation: Cardiovascular Imaging, 2014, 7, 20-30.	2.6	27
59	Gene-specific increase in the energetic cost of contraction in hypertrophic cardiomyopathy caused by thick filament mutations. Cardiovascular Research, 2014, 103, 248-257.	3.8	88
60	Validation of simplified dosimetry approaches in 89 Zr-PET/CT: The use of manual versus semi-automatic delineation methods to estimate organ absorbed doses. Medical Physics, 2014, 41, 102503.	3.0	11
61	Amyloid and its association with default network integrity in Alzheimer's disease. Human Brain Mapping, 2014, 35, 779-791.	3.6	37
62	Parametric Methods for Quantification of 18F-FAZA Kinetics in Non–Small Cell Lung Cancer Patients. Journal of Nuclear Medicine, 2014, 55, 1772-1777.	5.0	12
63	Synthesis and initial preclinical evaluation of the P2X <sub>7</sub> receptor antagonist [ <sup>11</sup> C]Aâ€740003 as a novel tracer of neuroinflammation. Journal of Labelled Compounds and Radiopharmaceuticals, 2014, 57, 509-516.	1.0	70
64	Accuracy and precision of pseudo-continuous arterial spin labeling perfusion during baseline and hypercapnia: A head-to-head comparison with 150 H2O positron emission tomography. NeuroImage, 2014, 92, 182-192.	4.2	133
65	Effect of Type 2 Diabetes Mellitus on Epicardial Adipose Tissue Volume and Coronary Vasomotor Function. American Journal of Cardiology, 2014, 113, 90-97.	1.6	18
66	<i>In Vivo</i> Imaging as a Pharmacodynamic Marker. Clinical Cancer Research, 2014, 20, 2569-2577.	7.0	12
67	Assessment of Simplified Methods to Measure <sup>18</sup> F-FLT Uptake Changes in EGFR-Mutated Non–Small Cell Lung Cancer Patients Undergoing EGFR Tyrosine Kinase Inhibitor Treatment. Journal of Nuclear Medicine, 2014, 55, 1417-1423.	5.0	17
68	Quantification of 18F-Fluoride Kinetics: Evaluation of Simplified Methods. Journal of Nuclear Medicine, 2014, 55, 1122-1127.	5.0	23
69	Multicenter Harmonization of <sup>89</sup> Zr PET/CT Performance. Journal of Nuclear Medicine, 2014, 55, 264-267.	5.0	63
70	Impact of anatomical and functional severity of coronary atherosclerotic plaques on the transmural perfusion gradient: a [150]H2O PET study. European Heart Journal, 2014, 35, 2094-2105.	2.2	66
71	The need for quantitative PET in multicentre studies. Clinical and Translational Imaging, 2014, 2, 277-280.	2.1	3
72	Quantitative Assessment of MyocardialÂPerfusion in the Detection of Significant Coronary Artery Disease. Journal of the American College of Cardiology, 2014, 64, 1464-1475.	2.8	253

#	Article	IF	CITATIONS
73	Comparison of Simplified Parametric Methods for Visual Interpretation of <sup>11</sup> C-Pittsburgh Compound-B PET Images. Journal of Nuclear Medicine, 2014, 55, 1305-1307.	5.0	24
74	Synthesis and preclinical evaluation of carbon-11 labelled N-((5-(4-fluoro-2-[11C]methoxyphenyl)pyridin-3-yl)methyl)cyclopentanamine as a PET tracer for NR2B subunit-containing NMDA receptors. Nuclear Medicine and Biology, 2014, 41, 670-680.	0.6	15
75	(R)-[11C]PK11195 brain uptake as a biomarker of inflammation and antiepileptic drug resistance: Evaluation in a rat epilepsy model. Neuropharmacology, 2014, 85, 104-112.	4.1	37
76	Concordance Between Cerebrospinal Fluid Biomarkers and [11C]PIB PET in a Memory Clinic Cohort. Journal of Alzheimer's Disease, 2014, 41, 801-807.	2.6	109
77	In vivo measurements of blood flow and bone metabolism in osteoarthritis. Rheumatology International, 2013, 33, 959-963.	3.0	22
78	[11C]quinidine and [11C]laniquidar PET imaging in a chronic rodent epilepsy model: Impact of epilepsy and drug-responsiveness. Nuclear Medicine and Biology, 2013, 40, 764-775.	0.6	22
79	Cerebral Blood Flow and Glucose Metabolism in Appetite-Related Brain Regions in Type 1 Diabetic Patients After Treatment With Insulin Detemir and NPH Insulin. Diabetes Care, 2013, 36, 4050-4056.	8.6	14
80	Dopaminergic activity in Tourette syndrome and obsessive-compulsive disorder. European Neuropsychopharmacology, 2013, 23, 1423-1431.	0.7	133
81	ENerGetIcs in hypertrophic cardiomyopathy: traNslation between MRI, PET and cardiac myofilament function (ENGINE study). Netherlands Heart Journal, 2013, 21, 567-571.	0.8	15
82	Microglial activation in Alzheimer's disease: an (R)-[11C]PK11195 positron emission tomography study. Neurobiology of Aging, 2013, 34, 128-136.	3.1	145
83	Pulmonary 2â€Deoxyâ€2â€{ <sup>18</sup> F]â€Fluoroâ€Dâ€Glucose Uptake is Low in Treated Patients with Idic Pulmonary Arterial Hypertension. Pulmonary Circulation, 2013, 3, 647-653.	opathic	12
84	Positron Emission Tomography as a Method for Measuring Drug Delivery to Tumors in vivo: The Example of [11C]docetaxel. Frontiers in Oncology, 2013, 3, 208.	2.8	23
85	Radiation Dose of the P-Glycoprotein Tracer <sup>11</sup> C-Laniquidar. Journal of Nuclear Medicine, 2013, 54, 2101-2103.	5.0	12
86	<sup>11</sup> C-Acetate Clearance as an Index of Oxygen Consumption of the Right Myocardium in Idiopathic Pulmonary Arterial Hypertension: A Validation Study Using <sup>15</sup> O-Labeled Tracers and PET. Journal of Nuclear Medicine, 2013, 54, 1258-1262.	5.0	18
87	Toward Prediction of Efficacy of Chemotherapy: A Proof of Concept Study in Lung Cancer Patients Using [11C]docetaxel and Positron Emission Tomography. Clinical Cancer Research, 2013, 19, 4163-4173.	7.0	58
88	Cerebral Blood Flow and Glucose Metabolism Measured With Positron Emission Tomography Are Decreased in Human Type 1 Diabetes. Diabetes, 2013, 62, 2898-2904.	0.6	32
89	Hybrid Imaging Using Quantitative H <sub>2</sub> <sup>15</sup> O PET and CT-Based Coronary Angiography for the Detection of Coronary Artery Disease. Journal of Nuclear Medicine, 2013, 54, 55-63.	5.0	109
90	Longitudinal Amyloid Imaging Using <sup>11</sup> C-PiB: Methodologic Considerations. Journal of Nuclear Medicine, 2013, 54, 1570-1576.	5.0	148

#	Article	IF	CITATIONS
91	<sup>11</sup> C″abeled and <sup>18</sup> F″abeled PET ligands for subtypeâ€specific imaging of histamine receptors in the brain. Journal of Labelled Compounds and Radiopharmaceuticals, 2013, 56, 120-129.	1.0	21
92	Development of [11C]erlotinib Positron Emission Tomography for <i>In Vivo</i> Evaluation of EGF Receptor Mutational Status. Clinical Cancer Research, 2013, 19, 183-193.	7.0	117
93	Limbic and motor circuits involved in symmetry behavior in Tourette's syndrome. CNS Spectrums, 2013, 18, 34-42.	1.2	16
94	Prognostic Impact of [18F]Fluorothymidine and [18F]Fluoro-D-Glucose Baseline Uptakes in Patients with Lung Cancer Treated First-Line with Erlotinib. PLoS ONE, 2013, 8, e53081.	2.5	36
95	In vivo quantification of striatal dopamine D <sub>2</sub> receptor occupancy by JNJ-37822681 using [ <sup>11</sup> C]raclopride and positron emission tomography. Journal of Psychopharmacology, 2012, 26, 1128-1135.	4.0	17
96	Amyloid burden and metabolic function in early-onset Alzheimer's disease: parietal lobe involvement. Brain, 2012, 135, 2115-2125.	7.6	109
97	Blood–brain barrier P-glycoprotein function in Alzheimer's disease. Brain, 2012, 135, 181-189.	7.6	252
98	Optimization of Supervised Cluster Analysis for Extracting Reference Tissue Input Curves in ( <i>R</i> )-[ <sup>11</sup> C]PK11195 Brain PET Studies. Journal of Cerebral Blood Flow and Metabolism, 2012, 32, 1600-1608.	4.3	120
99	Parametric [11C]flumazenil images. Nuclear Medicine Communications, 2012, 33, 422-430.	1.1	9
100	Tumor Lesion Glycolysis and Tumor Lesion Proliferation for Response Prediction and Prognostic Differentiation in Patients With Advanced Non–Small Cell Lung Cancer Treated With Erlotinib. Clinical Nuclear Medicine, 2012, 37, 1058-1064.	1.3	47
101	Altered GABA <sub>A</sub> Receptor Density and Unaltered Blood–Brain Barrier Transport in a Kainate Model of Epilepsy: An In Vivo Study Using <sup>11</sup> C-Flumazenil and PET. Journal of Nuclear Medicine, 2012, 53, 1974-1983.	5.0	26
102	No Evidence for Additional Blood–Brain Barrier P-Glycoprotein Dysfunction in Alzheimer's Disease Patients with Microbleeds. Journal of Cerebral Blood Flow and Metabolism, 2012, 32, 1468-1471.	4.3	18
103	Microglial activation in healthy aging. Neurobiology of Aging, 2012, 33, 1067-1072.	3.1	125
104	Synthesis and preclinical evaluation of [11C]D617, a metabolite of (R)-[11C]verapamil. Nuclear Medicine and Biology, 2012, 39, 530-539.	0.6	16
105	Quantitative relationship between coronary artery calcium score and hyperemic myocardial blood flow as assessed by hybrid 15O-water PET/CT imaging in patients evaluated for coronary artery disease. Journal of Nuclear Cardiology, 2012, 19, 256-264.	2.1	17
106	Rapid Decrease in Delivery of Chemotherapy to Tumors after Anti-VEGF Therapy: Implications for Scheduling of Anti-Angiogenic Drugs. Cancer Cell, 2012, 21, 82-91.	16.8	307
107	Reproducibility of quantitative (R)-[11C]verapamil studies. EJNMMI Research, 2012, 2, 1.	2.5	45
108	Macrophage positron emission tomography imaging as a biomarker for preclinical rheumatoid arthritis: Findings of a prospective pilot study. Arthritis and Rheumatism, 2012, 64, 62-66.	6.7	95

#	Article	IF	CITATIONS
109	Carriers of the hypertrophic cardiomyopathy MYBPC3 mutation are characterized by reduced myocardial efficiency in the absence of hypertrophy and microvascular dysfunction. European Journal of Heart Failure, 2011, 13, 1283-1289.	7.1	49
110	Simultaneous in vivo measurements of receptor density and affinity using [11C]flumazenil and positron emission tomography: Comparison of full saturation and steady state methods. NeuroImage, 2011, 57, 928-937.	4.2	9
111	Early Prediction of Nonprogression in Advanced Non–Small-Cell Lung Cancer Treated With Erlotinib By Using [ <sup>18</sup> F]Fluorodeoxyglucose and [ <sup>18</sup> F]Fluorothymidine Positron Emission Tomography. Journal of Clinical Oncology, 2011, 29, 1701-1708.	1.6	170
112	Reappraisal of a single-tissue compartment model for estimation of myocardial oxygen consumption by [11C]acetate PET. Nuclear Medicine Communications, 2011, 32, 59-62.	1.1	11
113	Relation of Coronary Microvascular Dysfunction in Hypertrophic Cardiomyopathy to Contractile Dysfunction Independent from Myocardial Injury. American Journal of Cardiology, 2011, 107, 1522-1528.	1.6	17
114	Feasibility of subendocardial and subepicardial myocardial perfusion measurements in healthy normals with 15O-labeled water and positron emission tomography. Journal of Nuclear Cardiology, 2011, 18, 650-656.	2.1	34
115	(R)-[11C]Verapamil PET studies to assess changes in P-glycoprotein expression and functionality in rat blood-brain barrier after exposure to kainate-induced status epilepticus. BMC Medical Imaging, 2011, 11, 1.	2.7	43
116	Systolic pulmonary artery pressure and heart rate are main determinants of oxygen consumption in the right ventricular myocardium of patients with idiopathic pulmonary arterial hypertension. European Journal of Heart Failure, 2011, 13, 1290-1295.	7.1	38
117	Absolute Quantification of [11C]docetaxel Kinetics in Lung Cancer Patients Using Positron Emission Tomography. Clinical Cancer Research, 2011, 17, 4814-4824.	7.0	19
118	Widespread and Prolonged Increase in ( <i>R</i> )- <sup>11</sup> C-PK11195 Binding After Traumatic Brain Injury. Journal of Nuclear Medicine, 2011, 52, 1235-1239.	5.0	72
119	Right Ventricular Failure in Idiopathic Pulmonary Arterial Hypertension Is Associated With Inefficient Myocardial Oxygen Utilization. Circulation: Heart Failure, 2011, 4, 700-706.	3.9	74
120	Parametric Images of Myocardial Viability Using a Single <sup>15</sup> O-H <sub>2</sub> O PET/CT Scan. Journal of Nuclear Medicine, 2011, 52, 745-749.	5.0	41
121	Effects of Image Characteristics on Performance of Tumor Delineation Methods: A Test–Retest Assessment. Journal of Nuclear Medicine, 2011, 52, 1550-1558.	5.0	60
122	<sup>18</sup> F-FDG PET as a Tool to Predict the Clinical Outcome of Infliximab Treatment of Rheumatoid Arthritis: An Explorative Study. Journal of Nuclear Medicine, 2011, 52, 77-80.	5.0	104
123	Quantitative Analysis of Response to Treatment with Erlotinib in Advanced Non–Small Cell Lung Cancer Using 18F-FDG and 3â€2-Deoxy-3â€2-18F-Fluorothymidine PET. Journal of Nuclear Medicine, 2011, 52, 1871-1877.	5.0	65
124	Myocardial Oxygen Extraction Fraction Measured Using Bolus Inhalation of <sup>15</sup> O-Oxygen Gas and Dynamic PET. Journal of Nuclear Medicine, 2011, 52, 60-66.	5.0	15
125	Cardiac PET-CT: advanced hybrid imaging for the detection of coronary artery disease. Netherlands Heart Journal, 2010, 18, 90-98.	0.8	62
126	Arterial Spin Labeling Perfusion MRI at Multiple Delay Times: A Correlative Study with H <sub>2</sub> <sup>15</sup> 0 Positron Emission Tomography in Patients with Symptomatic Carotid Artery Occlusion. Journal of Cerebral Blood Flow and Metabolism, 2010, 30, 222-229.	4.3	117

Adriaan A Lammertsma

#	Article	IF	CITATIONS
127	<i>In vivo</i> Validation of Reconstruction-Based Resolution Recovery for Human Brain Studies. Journal of Cerebral Blood Flow and Metabolism, 2010, 30, 381-389.	4.3	28
128	Low-Dose Quantitative Myocardial Blood Flow Imaging Using <sup>15</sup> O-Water and PET Without Attenuation Correction. Journal of Nuclear Medicine, 2010, 51, 575-580.	5.0	54
129	Liver Fat Content in Type 2 Diabetes: Relationship With Hepatic Perfusion and Substrate Metabolism. Diabetes, 2010, 59, 2747-2754.	0.6	37
130	Quantitative Parametric Perfusion Images Using <sup>15</sup> O-Labeled Water and a Clinical PET/CT Scanner: Test–Retest Variability in Lung Cancer. Journal of Nuclear Medicine, 2010, 51, 1684-1690.	5.0	42
131	Risk stratification for ventricular arrhythmias in ischaemic cardiomyopathy: the value of non-invasive imaging. Europace, 2010, 12, 468-474.	1.7	16
132	Carbon-11 Labeled Tracers for In Vivo Imaging of P-Glycoprotein Function: Kinetics, Advantages and Disadvantages. Current Topics in Medicinal Chemistry, 2010, 10, 1820-1833.	2.1	21
133	Effects of Hepatic Triglyceride Content on Myocardial Metabolism in Type 2 Diabetes. Journal of the American College of Cardiology, 2010, 56, 225-233.	2.8	108
134	Potential of [11C]acetate for measuring myocardial blood flow: Studies in normal subjects and patients with hypertrophic cardiomyopathy. Journal of Nuclear Cardiology, 2010, 17, 264-275.	2.1	25
135	Simplified parametric methods for [18F]FDDNP studies. NeuroImage, 2010, 49, 433-441.	4.2	7
136	Relationship of Cerebrospinal Fluid Markers to <sup>11</sup> C-PiB and <sup>18</sup> F-FDDNP Binding. Journal of Nuclear Medicine, 2009, 50, 1464-1470.	5.0	162
137	î"9-Tetrahydrocannabinol Induces Dopamine Release in the Human Striatum. Neuropsychopharmacology, 2009, 34, 759-766.	5.4	341
138	Detection of Alzheimer Pathology In Vivo Using Both <sup>11</sup> C-PIB and <sup>18</sup> F-FDDNP PET. Journal of Nuclear Medicine, 2009, 50, 191-197.	5.0	119
139	HRRT Versus HR+ Human Brain PET Studies: An Interscanner Test–Retest Study. Journal of Nuclear Medicine, 2009, 50, 693-702.	5.0	59
140	Accuracy of 3-Dimensional Reconstruction Algorithms for the High-Resolution Research Tomograph. Journal of Nuclear Medicine, 2009, 50, 72-80.	5.0	40
141	Comparison of transcranial Doppler ultrasonography and positron emission tomography using a three-dimensional template of the middle cerebral artery. Neurological Research, 2009, 31, 52-59.	1.3	13
142	Downregulation of <sup>18</sup> F-FDG Uptake in PET as an Early Pharmacodynamic Effect in Treatment of Non–Small Cell Lung Cancer with the mTOR Inhibitor Everolimus. Journal of Nuclear Medicine, 2009, 50, 1815-1819.	5.0	29
143	Reference Tissue Models and Blood–Brain Barrier Disruption: Lessons from ( <i>R</i> )-[ <sup>11</sup> C]PK11195 in Traumatic Brain Injury. Journal of Nuclear Medicine, 2009, 50, 1975-1979.	5.0	24
144	Repeatability of <sup>18</sup> F-FDG PET in a Multicenter Phase I Study of Patients with Advanced Gastrointestinal Malignancies. Journal of Nuclear Medicine, 2009, 50, 1646-1654.	5.0	129

#	Article	IF	CITATIONS
145	Pioglitazone Improves Cardiac Function and Alters Myocardial Substrate Metabolism Without Affecting Cardiac Triglyceride Accumulation and High-Energy Phosphate Metabolism in Patients With Well-Controlled Type 2 Diabetes Mellitus. Circulation, 2009, 119, 2069-2077.	1.6	210
146	No Signs of Metabolic Hyperactivity in Patients With Unilateral Condylar Hyperactivity: An In Vivo Positron Emission Tomography Study. Journal of Oral and Maxillofacial Surgery, 2009, 67, 576-581.	1.2	31
147	Coronary microvascular resistance: methods for its quantification in humans. Basic Research in Cardiology, 2009, 104, 485-498.	5.9	86
148	First Evaluation of [11C]R116301 as an In Vivo Tracer of NK1 Receptors in Man. Molecular Imaging and Biology, 2009, 11, 241-245.	2.6	8
149	Reproducibility of quantitative 18F-3′-deoxy-3′-fluorothymidine measurements using positron emission tomography. European Journal of Nuclear Medicine and Molecular Imaging, 2009, 36, 389-395.	6.4	71
150	Changes in GABA <sub>A</sub> receptor properties in amygdala kindled animals: In vivo studies using [ <sup>11</sup> C]flumazenil and positron emission tomography. Epilepsia, 2009, 50, 88-98.	5.1	43
151	Hemodynamic changes in ipsi- and contralateral cerebral arterial territories after carotid endarterectomy using positron emission tomography. World Neurosurgery, 2009, 71, 668-676.	1.3	9
152	Evaluation of [11C]laniquidar as a tracer of P-glycoprotein: radiosynthesis and biodistribution in rats. Nuclear Medicine and Biology, 2009, 36, 643-649.	0.6	66
153	Synthesis of 2-(1,1-dicyanopropen-2-yl)-6-(2-[18F]-fluoroethyl)-methylamino-naphthalene ([18F]FDDNP). Applied Radiation and Isotopes, 2008, 66, 203-207.	1.5	13
154	[18F]FDG and [18F]FLT uptake in human breast cancer cells in relation to the effects of chemotherapy: an in vitro study. British Journal of Cancer, 2008, 99, 481-487.	6.4	40
155	Comparison of Plasma Input and Reference Tissue Models for Analysing [ <sup>11</sup> C]flumazenil Studies. Journal of Cerebral Blood Flow and Metabolism, 2008, 28, 579-587.	4.3	52
156	Gap Filling Strategies for 3-D-FBP Reconstructions of High-Resolution Research Tomograph Scans. IEEE Transactions on Medical Imaging, 2008, 27, 934-942.	8.9	24
157	Microglia Activation in Recent-Onset Schizophrenia: A Quantitative (R)-[11C]PK11195 Positron Emission Tomography Study. Biological Psychiatry, 2008, 64, 820-822.	1.3	534
158	Peripheral metabolism of [18F]FDDNP and cerebral uptake of its labelled metabolites. Nuclear Medicine and Biology, 2008, 35, 869-874.	0.6	24
159	Blood–brain barrier P-glycoprotein function is not impaired in early Parkinson's disease. Parkinsonism and Related Disorders, 2008, 14, 505-508.	2.2	57
160	Reduced GABAA benzodiazepine receptor binding in veterans with post-traumatic stress disorder. Molecular Psychiatry, 2008, 13, 74-83.	7.9	148
161	Partial volume corrected image derived input functions for dynamic PET brain studies: Methodology and validation for [11C]flumazenil. NeuroImage, 2008, 39, 1041-1050.	4.2	127
162	Simplified parametric methods for [11C]PIB studies. NeuroImage, 2008, 42, 76-86.	4.2	85

#	Article	IF	CITATIONS
163	Image derived input functions for dynamic High Resolution Research Tomograph PET brain studies. NeuroImage, 2008, 43, 676-686.	4.2	37
164	Quantitative Issues in Response Measurement by PET. PET Clinics, 2008, 3, 5-11.	3.0	2
165	A new rat model of human breast cancer for evaluating efficacy of new anti-cancer agents in vivo. Cancer Biology and Therapy, 2008, 7, 532-537.	3.4	10
166	Reproducibility of Tumor Perfusion Measurements Using <sup>15</sup> O-Labeled Water and PET. Journal of Nuclear Medicine, 2008, 49, 1763-1768.	5.0	44
167	Impact of wavelet based denoising of â€PK11195 time activity curves on accuracy and precision of kinetic analysis. Medical Physics, 2008, 35, 5069-5078.	3.0	1
168	Individualized Treatment Planning in Oncology: Role of PET and Radiolabelled Anticancer Drugs in Predicting Tumour Resistance. Current Pharmaceutical Design, 2008, 14, 2914-2931.	1.9	29
169	Hyperaemic microvascular resistance is not increased in viable myocardium after chronic myocardial infarction. European Heart Journal, 2007, 28, 2320-2325.	2.2	30
170	Microvascular Function in Viable Myocardium After Chronic Infarction Does Not Influence Fractional Flow Reserve Measurements. Journal of Nuclear Medicine, 2007, 48, 1987-1992.	5.0	28
171	Myocardial Energetics and Efficiency. Circulation, 2007, 115, 918-927.	1.6	168
172	SPM analysis of parametric (R)-[11C]PK11195 binding images: Plasma input versus reference tissue parametric methods. NeuroImage, 2007, 35, 1473-1479.	4.2	26
173	Evaluation of Tracer Kinetic Models for Quantification of P-Glycoprotein Function using (R)-[11C]Verapamil and PET. Journal of Cerebral Blood Flow and Metabolism, 2007, 27, 424-433.	4.3	87
174	Quantification of Dopamine Transporter Binding Using [18F]FP-β-CIT and Positron Emission Tomography. Journal of Cerebral Blood Flow and Metabolism, 2007, 27, 1397-1406.	4.3	34
175	Evaluation of Methods for Generating Parametric (R)-[11C]PK11195 Binding Images. Journal of Cerebral Blood Flow and Metabolism, 2007, 27, 1603-1615.	4.3	32
176	Evaluation of Reference Regions for <i>(R)</i> -[ <sup>11</sup> C]PK11195 Studies in Alzheimer's Disease and Mild Cognitive Impairment. Journal of Cerebral Blood Flow and Metabolism, 2007, 27, 1965-1974.	4.3	53
177	Consensus Nomenclature for in vivo Imaging of Reversibly Binding Radioligands. Journal of Cerebral Blood Flow and Metabolism, 2007, 27, 1533-1539.	4.3	1,840
178	Quantification of Myocardial Perfusion Using Intravenous Myocardial Contrast Echocardiography in Healthy Volunteers: Comparison with Positron Emission Tomography. Journal of the American Society of Echocardiography, 2006, 19, 285-293.	2.8	31
179	Performance of Immuno–Positron Emission Tomography with Zirconium-89-Labeled Chimeric Monoclonal Antibody U36 in the Detection of Lymph Node Metastases in Head and Neck Cancer Patients. Clinical Cancer Research, 2006, 12, 2133-2140.	7.0	207
180	Radiosynthesis and biodistribution of a histamine H3 receptor antagonist 4-[3-(4-piperidin-1-yl-but-1-ynyl)-[11C]benzyl]-morpholine: evaluation of a potential PET ligand. Nuclear Medicine and Biology, 2006, 33, 801-810.	0.6	29

#	Article	IF	CITATIONS
181	Different brain effects during chronic and acute sacral neuromodulation in urge incontinent patients with implanted neurostimulators. BJU International, 2006, 98, 1238-1243.	2.5	183
182	Evaluation of Reference Tissue Models for the Analysis of [11C](R)-PK11195 Studies. Journal of Cerebral Blood Flow and Metabolism, 2006, 26, 1431-1441.	4.3	145
183	Effect of age on functional P-glycoprotein in the blood-brain barrier measured by use of (R)-[11C]verapamil and positron emission tomography. Clinical Pharmacology and Therapeutics, 2006, 79, 540-548.	4.7	163
184	Regional heterogeneity of resting perfusion in hypertrophic cardiomyopathy is related to delayed contrast enhancement but not to systolic function: A PET and MRI study. Journal of Nuclear Cardiology, 2006, 13, 660-667.	2.1	35
185	How should we analyse FDG PET studies for monitoring tumour response?. European Journal of Nuclear Medicine and Molecular Imaging, 2006, 33, 16-21.	6.4	67
186	Does Myocardial Fibrosis Hinder Contractile Function and Perfusion in Idiopathic Dilated Cardiomyopathy? PET and MR Imaging Study. Radiology, 2006, 240, 380-388.	7.3	51
187	Asymptomatic Carotid Artery Stenosis: Past, Present and Future. European Neurology, 2006, 56, 139-154.	1.4	28
188	Measurement of left ventricular volumes and function with O-15–labeled carbon monoxide gated positron emission tomography: Comparison with magnetic resonance imaging. Journal of Nuclear Cardiology, 2005, 12, 639-644.	2.1	19
189	Population plasma pharmacokinetics of 11C-flumazenil at tracer concentrations. British Journal of Clinical Pharmacology, 2005, 60, 477-485.	2.4	13
190	Development of a Tracer Kinetic Plasma Input Model for (R)-[11C]PK11195 Brain Studies. Journal of Cerebral Blood Flow and Metabolism, 2005, 25, 842-851.	4.3	68
191	Effects of ROI definition and reconstruction method on quantitative outcome and applicability in a response monitoring trial. European Journal of Nuclear Medicine and Molecular Imaging, 2005, 32, 294-301.	6.4	247
192	Prognostic Relevance of Response Evaluation Using [ <sup>18</sup> F]-2-Fluoro-2-Deoxy-D-Glucose Positron Emission Tomography in Patients With Locally Advanced Non–Small-Cell Lung Cancer. Journal of Clinical Oncology, 2005, 23, 8362-8370.	1.6	243
193	Memory Performance and the Growth Hormone/Insulin-Like Growth Factor Axis in Elderly: A Positron Emission Tomography Study. Neuroendocrinology, 2005, 81, 31-40.	2.5	37
194	Evaluation of (R)-[11C]verapamil as PET tracer of P-glycoprotein function in the blood–brain barrier: kinetics and metabolism in the rat. Nuclear Medicine and Biology, 2005, 32, 87-93.	0.6	102
195	Optimizing an online SPE–HPLC method for analysis of (R)-[11C]1-(2-chlorophenyl)-N-methyl-N-(1-methylpropyl)-3-isoquinolinecarboxamide [(R)-[11C]PK11195] and its metabolites in humans. Nuclear Medicine and Biology, 2005, 32, 307-312.	0.6	29
196	Effects of Cardiac Resynchronization Therapy on Myocardial Perfusion Reserve. Circulation, 2004, 110, 646-651.	1.6	115
197	18F-2-Fluoro-2-Deoxy-d-Glucose Positron Emission Tomography in Staging of Locally Advanced Breast Cancer. Journal of Clinical Oncology, 2004, 22, 1253-1259.	1.6	121
198	Amygdala activity in obsessive-compulsive disorder with contamination fear: a study with oxygen-15 water positron emission tomography. Psychiatry Research - Neuroimaging, 2004, 132, 225-237.	1.8	98

#	Article	IF	CITATIONS
199	Neurophysiological correlates of habituation during exposure in spider phobia. Psychiatry Research - Neuroimaging, 2004, 132, 149-158.	1.8	47
200	Correction for emission contamination in transmission scans for the high resolution research tomograph. IEEE Transactions on Nuclear Science, 2004, 51, 673-676.	2.0	9
201	Measuring [18F]FDG uptake in breast cancer during chemotherapy: comparison of analytical methods. European Journal of Nuclear Medicine and Molecular Imaging, 2003, 30, 674-681.	6.4	80
202	The perfusable tissue index: a marker of myocardial viability. Journal of Nuclear Cardiology, 2003, 10, 684-691.	2.1	21
203	18 FDG positron emission tomography versus 67 Ga scintigraphy as prognostic test during chemotherapy for non-Hodgkin's lymphoma. British Journal of Haematology, 2003, 123, 454-462.	2.5	37
204	Myocardial viability inchronic ischemic heart disease. Journal of the American College of Cardiology, 2003, 41, 1341-1348.	2.8	181
205	Experimental evaluation of iterative reconstruction versus filtered back projection for 3D [150]water PET activation studies using statistical parametric mapping analysis. NeuroImage, 2003, 19, 1170-1179.	4.2	21
206	Attenuation correction of PET activation studies in the presenceof task-related motion. NeuroImage, 2003, 19, 1501-1509.	4.2	21
207	Effects of attenuation correction and reconstruction method on PET activation studies. NeuroImage, 2003, 20, 898-908.	4.2	12
208	(R)- and (S)-[11C]verapamil as PET-tracers for measuring P-glycoprotein function: in vitro and in vivo evaluation. Nuclear Medicine and Biology, 2003, 30, 747-751.	0.6	106
209	Correction methods for missing data in sinograms of the HRRT PET scanner. IEEE Transactions on Nuclear Science, 2003, 50, 1452-1456.	2.0	34
210	Matching PET and CT scans of the head and neck area: Development of method and validation. Medical Physics, 2002, 29, 2230-2238.	3.0	29
211	Determinants of Diagnostic Performance Of [F-18]Fluorodeoxyglucose Positron Emission Tomography for Axillary Staging in Breast Cancer. Annals of Surgery, 2002, 236, 619-624.	4.2	92
212	Radioligand studies: imaging and quantitative analysis. European Neuropsychopharmacology, 2002, 12, 513-516.	0.7	48
213	PET/SPECT: functional imaging beyond flow. Vision Research, 2001, 41, 1277-1281.	1.4	35
214	Characteristics of a new fully programmable blood sampling device for monitoring blood radioactivity during PET. European Journal of Nuclear Medicine and Molecular Imaging, 2001, 28, 81-89.	2.1	136
215	Pulmonary β adrenoceptor density in arrhythmogenic right ventricular cardiomyopathy and idiopathic tachycardia. Basic Research in Cardiology, 2001, 96, 91-97.	5.9	13
216	Dipyridamole-induced increased glucose uptake in patients with single-vessel coronary artery disease assessed with PET. Journal of Nuclear Cardiology, 2001, 8, 339-346.	2.1	30

Adriaan A Lammertsma

#	Article	IF	CITATIONS
217	Carbon-11 acetate as a tracer of myocardial oxygen consumption. European Journal of Nuclear Medicine and Molecular Imaging, 2001, 28, 651-668.	2.1	78
218	Abnormalities of Cardiac Sympathetic Innervation in Arrhythmogenic Right Ventricular Cardiomyopathy. Circulation, 2000, 101, 1552-1558.	1.6	145
219	Quantitative analysis of [carbonyl-11C]WAY-100635 PET studies. Nuclear Medicine and Biology, 2000, 27, 477-482.	0.6	46
220	Transmural myocardial blood flow distribution in hypertrophic cardiomyopathy and effect of treatment. Basic Research in Cardiology, 1999, 94, 49-59.	5.9	72
221	Evaluation of compartmental and spectral analysis models of [/sup 18/F]FDG kinetics for heart and brain studies with PET. IEEE Transactions on Biomedical Engineering, 1998, 45, 1429-1448.	4.2	55
222	Cardiac sympathetic innervation in patients with idiopathic right ventricular outflow tract tachycardia. Journal of the American College of Cardiology, 1998, 32, 181-186.	2.8	104
223	Tracer Kinetic Modeling of the 5-HT1AReceptor Ligand [carbonyl-11C]WAY-100635 for PET. NeuroImage, 1998, 8, 426-440.	4.2	267
224	Myocardial Presynaptic and Postsynaptic Autonomic Dysfunction in Hypertrophic Cardiomyopathy. Circulation Research, 1998, 82, 57-62.	4.5	155
225	Parametric Imaging of Ligand-Receptor Binding in PET Using a Simplified Reference Region Model. NeuroImage, 1997, 6, 279-287.	4.2	998
226	In vivo saturation kinetics of two dopamine transporter probes measured using a small animal positron emission tomography scanner. Journal of Neuroscience Methods, 1997, 76, 45-51.	2.5	32
227	Pathophysiological Mechanisms of Chronic Reversible Left Ventricular Dysfunction due to Coronary Artery Disease (Hibernating Myocardium). Circulation, 1997, 96, 3205-3214.	1.6	132
228	Development of central 5-HT2A receptor radioligands for PET: Comparison of [3H]RP 62203 and [3H]SR 46349B kinetics in rat brain. Nuclear Medicine and Biology, 1996, 23, 245-250.	0.6	12
229	Simplified Reference Tissue Model for PET Receptor Studies. NeuroImage, 1996, 4, 153-158.	4.2	1,864
230	Measurement of liver blood flow using oxygen-15 labelled water and dynamic positron emission tomography: Limitations of model description. European Journal of Nuclear Medicine and Molecular Imaging, 1996, 23, 169-177.	2.1	48
231	Comparison of Methods for Analysis of Clinical [11C]Raclopride Studies. Journal of Cerebral Blood Flow and Metabolism, 1996, 16, 42-52.	4.3	441
232	Noninvasive Quantification of rCBF Using Positron Emission Tomography. Journal of Cerebral Blood Flow and Metabolism, 1996, 16, 311-319.	4.3	37
233	Linear dimension reduction of sequences of medical images: III. Factor analysis in signal space. Physics in Medicine and Biology, 1996, 41, 1469-1481.	3.0	14
234	Noninvasive Quantification of Regional Myocardial Metabolic Rate of Oxygen by <sup>15</sup> O <sub>2</sub> Inhalation and Positron Emission Tomography. Circulation, 1996, 94, 808-816.	1.6	47

#	Article	IF	CITATIONS
235	Hyperdynamic performance of remote myocardium in acute infarction. European Heart Journal, 1995, 16, 1845-1850.	2.2	26
236	Benzodiazepine-GABAA Receptors in Idiopathic Generalized Epilepsy Measured with [11C]Flumazenil and Positron Emission Tomography. Epilepsia, 1995, 36, 113-121.	5.1	47
237	Benzodiazepine-GABAA Receptor Binding During Absence Seizures. Epilepsia, 1995, 36, 592-599.	5.1	28
238	Effect of tissue heterogeneity on quantification in positron emission tomography. European Journal of Nuclear Medicine and Molecular Imaging, 1995, 22, 652-663.	2.1	23
239	Effect of Lâ€dopa and 6â€hydroxydopamine lesioning on [ <sup>11</sup> C]raclopride binding in rat striatum, quantified using PET. Synapse, 1995, 21, 45-53.	1.2	91
240	Benzodiazepine Receptor Quantification in vivo in Humans Using [ <sup>11</sup> C]Flumazenil and PET: Application of the Steady-State Principle. Journal of Cerebral Blood Flow and Metabolism, 1995, 15, 152-165.	4.3	204
241	Dosimetry of intravenously administered oxygen-15 labelled water in man: a model based on experimental human data from 21 subjects. European Journal of Nuclear Medicine and Molecular Imaging, 1994, 21, 1126-34.	2.1	33
242	Dose dependent occupancy of central dopamine D2 receptors by the novel neuroleptic CP-88,059-01: a study using positron emission tomography and11C-raclopride. Psychopharmacology, 1993, 112, 308-314.	3.1	97
243	Diffuse reduction of myocardial beta-adrenoceptors in hypertrophic cardiomyopathy: A study with positron emission tomography. Journal of the American College of Cardiology, 1993, 22, 1653-1660.	2.8	91
244	Comparison of regional myocardial blood flow in syndrome X and one-vessel coronary artery disease. American Journal of Cardiology, 1993, 72, 134-139.	1.6	97
245	Vasodilator reserve in collateral-dependent myocardium as measured by positron emission tomography. European Heart Journal, 1993, 14, 336-343.	2.2	37
246	Changes in global cerebral blood flow in humans: effect on regional cerebral blood flow during a neural activation task Journal of Physiology, 1993, 471, 521-534.	2.9	116
247	Measurement of regional myocardial blood flow using C 15 O 2 and positron emission tomography: comparison of tracer models. Clinical Physics and Physiological Measurement: an Official Journal of the Hospital Physicists' Association, Deutsche Gesellschaft Fur Medizinische Physik and the European Federation of Organisations for Medical Physics, 1992, 13, 1-20.	0.5	29
248	Dipyridamole vasodilator response after human orthotopic heart transplantation: Quantification by oxygen-15-labeled water and positron emission tomography. Journal of the American College of Cardiology, 1992, 19, 100-106.	2.8	46
249	Low oxygen extraction fraction in tumours measured with the oxygen-15 steady state technique: effect of tissue heterogeneity. British Journal of Radiology, 1992, 65, 697-700.	2.2	31
250	Quantitation of Carbon-11-labeled raclopride in rat striatum using positron emission tomography. Synapse, 1992, 12, 47-54.	1.2	198
251	In vivo Measurement of the Volume of Distribution of Water in Cerebral Grey Matter: Effects on the Calculation of Regional Cerebral Blood Flow. Journal of Cerebral Blood Flow and Metabolism, 1992, 12, 291-295.	4.3	16
252	Positron emission tomography. Brain Topography, 1992, 5, 113-117.	1.8	11

#	Article	IF	CITATIONS
253	Regional cerebral blood flow during volitional breathing in man Journal of Physiology, 1991, 443, 91-103.	2.9	186
254	Measurement of Cerebral Monoamine Oxidase B Activity Using L-[11C]Deprenyl and Dynamic Positron Emission Tomography. Journal of Cerebral Blood Flow and Metabolism, 1991, 11, 545-556.	4.3	72
255	Quantitative measurement of monoclonal antibody distribution and blood flow using positron emission tomography and124iodine in patients with breast cancer. International Journal of Cancer, 1991, 47, 344-347.	5.1	66
256	Measurement of human cerebral monoamine oxidase type B (MAO-B) activity with positron emission tomography (PET): a dose ranging study with the reversible inhibitor Ro 19-6327. European Journal of Clinical Pharmacology, 1991, 40, 169-173.	1.9	90
257	Noninvasive quantification of regional myocardial blood flow in coronary artery disease with oxygen-15-labeled carbon dioxide inhalation and positron emission tomography Circulation, 1991, 83, 875-885.	1.6	259
258	Combination of Dynamic and Integral Methods for Generating Reproducible Functional CBF Images. Journal of Cerebral Blood Flow and Metabolism, 1990, 10, 675-686.	4.3	137
259	The Relationship between Global and Local Changes in PET Scans. Journal of Cerebral Blood Flow and Metabolism, 1990, 10, 458-466.	4.3	841
260	Use of PET Methods for Measurement of Cerebral Energy Metabolism and Hemodynamics in Cerebrovascular Disease. Journal of Cerebral Blood Flow and Metabolism, 1989, 9, 723-742.	4.3	161
261	The C <sup>15</sup> O <sub>2</sub> Build-up Technique to Measure Regional Cerebral Blood Flow and Volume of Distribution of Water. Journal of Cerebral Blood Flow and Metabolism, 1989, 9, 461-470.	4.3	59
262	The colour centre in the cerebral cortex of man. Nature, 1989, 340, 386-389.	27.8	479
263	Stability of Arterial Concentrations during Continuous Inhalation of C15O2 and 15O2 and the Effects on Computed Values of CBF and CMRO2. Journal of Cerebral Blood Flow and Metabolism, 1988, 8, 411-417.	4.3	8
264	Rubidium-82 Myocardial Uptake and Extraction After Transient Ischemia. Journal of Computer Assisted Tomography, 1987, 11, 60-66.	0.9	24
265	Positron emission tomography andin vivo measurements of tumour perfusion and oxygen utilisation. Cancer and Metastasis Reviews, 1987, 6, 521-539.	5.9	10
266	Measurement of Glucose Utilisation with [18F]2-Fluoro-2-Deoxy-D-Glucose: A Comparison of Different Analytical Methods. Journal of Cerebral Blood Flow and Metabolism, 1987, 7, 161-172.	4.3	76
267	Correction for Intravascular Activity in the Oxygen-15 Steady-State Technique is Independent of the Regional Hematocrit. Journal of Cerebral Blood Flow and Metabolism, 1987, 7, 372-374.	4.3	31
268	Studies on regional cerebral haematocrit and blood flow in patients with cerebral tumours using positron emission tomography. Microvascular Research, 1986, 31, 267-276.	2.5	19
269	Measurement of regional cerebral blood flow, blood volume and oxygen metabolism in patients with sickle cell disease using positron emission tomography Stroke, 1986, 17, 692-698.	2.0	97
270	Glucose Transport across the Blood—Brain Barrier in Normal Human Subjects and Patients with Cerebral Tumours Studied Using [11C]3-O-Methyl-D-Glucose and Positron Emission Tomography. Journal of Cerebral Blood Flow and Metabolism, 1986, 6, 230-239.	4.3	51

#	Article	IF	CITATIONS
271	A comparison between regional cerebral blood flow measurements obtained in human subjects using <sup>11</sup> C-methylalbumin microspheres, the C <sup>15</sup> O <sub>2</sub> steady-state method, and positron emission tomography. Acta Neurologica Scandinavica, 1986, 73, 415-422.	2.1	18
272	Measurement of blood flow, oxygen utilisation, oxygen extraction ratio, and fractional blood volume in human brain tumours and surrounding oedematous tissue. British Journal of Radiology, 1985, 58, 725-734.	2.2	77
273	Measurement of Cerebral Blood Flow Using Bolus Inhalation of C <sup>15</sup> O <sub>2</sub> and Positron Emission Tomography: Description of the Method and its Comparison with the C <sup>15</sup> O <sub>2</sub> Continuous Inhalation Method. Journal of Cerebral Blood Flow and Metabolism. 1984. 4. 224-234.	4.3	76
274	In vivo Measurement of Regional Cerebral Haematocrit Using Positron Emission Tomography. Journal of Cerebral Blood Flow and Metabolism, 1984, 4, 317-322.	4.3	145
275	Measurement of Regional Cerebral pH in Human Subjects Using Continuous Inhalation of 11CO2 and Positron Emission Tomography. Journal of Cerebral Blood Flow and Metabolism, 1984, 4, 458-465.	4.3	58
276	A Method to Quantitate the Fractional Extraction of Rubidium-82 across the Blood—Brain Barrier Using Positron Emission Tomography. Journal of Cerebral Blood Flow and Metabolism, 1984, 4, 523-534.	4.3	32
277	Quantitative Measurement of Blood—Brain Barrier Permeability Using Rubidium-82 and Positron Emission Tomography. Journal of Cerebral Blood Flow and Metabolism, 1984, 4, 535-545.	4.3	86
278	Correction for the Presence of Intravascular Oxygen-15 in the Steady-State Technique for Measuring Regional Oxygen Extraction Ratio in the Brain: 1. Description of the Method. Journal of Cerebral Blood Flow and Metabolism, 1983, 3, 416-424.	4.3	297
279	In vivo measurements of regional cerebral blood flow and blood volume in patients with brain tumours using positron emission tomography. Acta Neurochirurgica, 1983, 69, 5-13.	1.7	40
280	A Statistical Study of the Steady State Technique for Measuring Regional Cerebral Blood Flow and Oxygen Utilisation Using 150. Journal of Computer Assisted Tomography, 1982, 6, 566-573.	0.9	59
281	Measurement of regional cerebral blood flow and oxygen utilisation in patients with cerebral tumours using 150 and positron emission tomography: Analytical techniques and preliminary results. Neuroradiology, 1982, 23, 63-74.	2.2	182
282	A Theoretical Study of the Steady-State Model for Measuring Regional Cerebral Blood Flow and Oxygen Utilisation Using Oxygen-15. Journal of Computer Assisted Tomography, 1981, 5, 544-550.	0.9	133
283	Extraction of Water Labeled With Oxygen 15 During Single-Capillary Transit. Archives of Neurology, 1981, 38, 581.	4.5	33